JOURNAL OF GEOPHYSICAL RESEARCH, VOL. 96, NO. A9, PAGES 15,943–15,949, SEPTEMBER 1, 1991

Mid-Latitude *E* Region Field-Aligned Irregularities Observed With the MU Radar

MAMORU YAMAMOTO,[1] SHOICHIRO FUKAO,[1] RONALD F. WOODMAN,[2]
TADAHIKO OGAWA,[3] TOSHITAKA TSUDA,[1] AND SUSUMU KATO[1]

Fine structures of *E* region field-aligned irregularities were observed on June 24–25, 1989, with the MU radar at Shigaraki, Japan (34.9°N, 136.1°E; geomagnetic latitude 25.0°N). The 3.2-m scale irregularities were observed with the MU radar in five main beam directions, each of which was nearly perpendicular to the geomagnetic field at 100 km altitude. Doppler spectra were obtained every 20 s with a range resolution of 600 m. Field-perpendicular echoes appeared from 2130 to 2330 LT and from 0400 to 1100 LT, times that correspond to postsunset and postsunrise period in the *E* region. A preliminary examination of the Doppler spectra indicates spectral widths of 50–120 m s^{-1} and the mean Doppler velocities are well below the ion acoustic speed. These spectral characteristics are consistent with those obtained in the equatorial and auroral electrojets, and have been attributed to the gradient drift instability. The echoes observed during the postsunset and postsunrise periods showed quite different morphologies in the time-height distribution. For this reason, they are classified into two types, "continuous" and "quasi-periodic." The appearance of the "continuous" echoes was mainly continuous in time and situated between 90 and 100 km altitude during the postsunrise period. The appearance of the "quasi-periodic" echoes was intermittent with periods of 5–10 min and situated above 100 km altitude during the postsunset period. The quasi-periodic echoes showed phase propagation toward the radar, while the averaged mean Doppler velocity was away from the radar. By measuring the time delays in echo regions from five directions, an apparent westward motion (approximately 120 m s^{-1}) of the irregularity regions was estimated.

1. INTRODUCTION

In the equatorial and auroral regions, many observations of field-aligned irregularities in the ionospheric *E* region have been conducted with a variety of techniques (see reviews by *Fejer and Kelley* [1980] and *Haldoupis* [1989]). In the mid-latitude region, however, the number of observations is limited: *Ecklund et al.* [1981] and *Riggin et al.* [1986] observed *E* region irregularities with 50-MHz radars near Arecibo, Puerto Rico, *Tanaka and Venkateswaran* [1982*a*, *b*] with a 25-MHz radar at Iioka, Japan (35.7°N, 140.8°E), and *Keys and Andrews* [1984] with three VHF radars in the south of New Zealand. The above investigations have revealed that the field-aligned irregularities are closely associated with sporadic *E* layers (detected, for example, by incoherent scatter radar), and appear to be generated by the gradient drift instability mechanism [*Simon*, 1963; *Kato*, 1972]. In all cases, however, the range resolution varied from 3 to 15 km; consequently, fine structures in the irregularities could not be fully analyzed.

The MU radar is a monostatic Doppler radar with a carrier frequency of 46.5 MHz and is located at Shigaraki, Japan (34.9°N, 136.1°E; geomagnetic latitude 25.0°N) [*Kato et al.*, 1984; *Fukao et al.*, 1985*a*, *b*]. By directing the antenna beam northward with zenith angles of 50°–60°, it is possible to achieve orthogonal intersection with geomagnetic field lines and, hence, to measure characteristics of 3.2-m field-aligned irregularities in both the *E* and the *F* regions. *Fukao et al.* [1988] conducted the first observations of *F* region field-aligned irregularities with the MU radar; detailed results of those observations were reported by *Fukao et al.* [1991] and *Kelley and Fukao* [1991]. *Fukao et al.* [1991] also presented the first MU radar observations of *E* region field-aligned irregularities. Because they used the same 4.8-km range resolution for both the *E* and the *F* region irregularity observations, it was difficult to examine the fine structure of the irregularities. In this paper, we report results of *E* region field-aligned irregularity observations with the MU radar by using five beam directions with a range resolution of 600 m.

2. EXPERIMENT DESCRIPTION

We conducted the MU radar observations of the *E* region irregularities on June 24–25, 1989, using the observation parameters listed in Table 1. The antenna beam was steered to each of the five specified azimuths successively every interpulse period (IPP), thus providing an azimuth coverage of ±10° about geographic north. We used the International Geomagnetic Reference Field model (IGRF85) to compute the zenith angle at which the boresight of the antenna beam was perpendicular to the geomagnetic field at the altitude of 100 km, as a function of azimuth angle [*Fukao et al.*, 1991]. The five beam directions were selected from the 1657 discrete directions allowed by the MU radar. As shown in Table 1, the selected beam directions were closest to those computed to achieve exact geomagnetic orthogonality; the differences between the model and the steered zenith angles ranged from 0.04° to 0.34°. The data range gates were set from 120 to 196 km which covered the altitude interval from 74 to 125 km. The two-way, half-power total antenna beam width was 4.5°/2.3° in the vertical/horizontal plane. The finite width of the beam assured that exact perpendicularity to the geomagnetic field could be obtained somewhere within the beam in the *E* region. Because the zenith angles used were

[1]Radio Atmospheric Science Center, Kyoto University, Uji, Kyoto, Japan.
[2]Radio Observatorio de Jicamarca, Instituto Geofisico del Peru, Lima.
[3]Hiraiso Solar Terrestrial Research Center, Communications Research Laboratory, Nakaminato, Ibaraki, Japan.

Paper number 91JA01321.
0148-0227/91/91JA-01321$05.00

TABLE 1. Observation Parameters of the MU Radar

Parameter	Value
Observation period	June 24–25, 1989
Range	120–196 km
Range resolution	600 m
Beam directions*	
Beam 1	(−9.35°, 50.92°, 50.86°)
Beam 2	(−4.14°, 50.89°, 50.85°)
Beam 3	(0.00°, 50.97°, 51.02°)
Beam 4	(5.41°, 51.68°, 51.48°)
Beam 5	(10.39°, 51.82°, 52.16°)
Beam width	
Vertical	4.5°
Horizontal	2.3°
Interpulse period	1500 μs
Number of FFT points	128
Number of incoherent integrations	10
Time resolution	20 s

FFT denotes fast Fourier transform.
*(steered azimuth angle, steered zenith angle, model zenith angle)

outside of the designed limit of 30°, two significant grating lobes existed in southward directions [*Fukao et al.*, 1990]. Considering that the aspect angle sensitivity is about 90° ± 1° for field-aligned irregularities [*Bowles et al.*, 1963; *Riggin et al.*, 1986], the southward directed grating lobes were so far from perpendicularity that they could be confidently ignored.

Because the beam direction was cyclically changed, each of five pulses was transmitted to a certain direction. Hence, the sampling interval was 7.5 ms for a time series constructed from data taken in one direction, which corresponds to the Nyquist limit of 66 Hz (the Doppler velocity of ±215 m s^{-1}). The Doppler power spectra of the received signal were calculated every 0.96 s using a 128-point fast Fourier transform, and were processed through 10 incoherent integrations. Including the time spent for computation and data transfer, averaged spectra were recorded on magnetic tape every 20 s. The descriptive parameters of the Doppler spectrum, i.e., echo power, mean Doppler velocity and spectral width, were estimated by the moment method. As shown by *Yamamoto et al.* [1988], the estimation error of the mean Doppler velocity is a function of the spectral width and observation period. Assuming an observation period of 9.6 s and a half-power full spectral width of 100 m s^{-1}, the estimation error of the mean Doppler velocity is approximately 1.5 m s^{-1} when the signal-to-noise ratio (snr) is larger than 0 dB.

3. Data Presentation

3.1. *General Description*

Figure 1 shows the Doppler spectra of the field-perpendicular echoes observed in beam 3 at 2140 LT on June 24, 1989. Intense echoes are found at 152–156 km range and 168–196 km range. The spectral peak reaches 40 dB above the noise level around 174 km range. Positive velocity corresponds to motion away from the radar. Although some aliasing of spectra is found at the range of 170–176 km, spectral peaks stay within the Nyquist limit of ±215 m s^{-1}. The mean Doppler velocity is well below the ion acoustic velocity (~300 m s^{-1}). The half-power full spectral width ranges between 50 and 120 m s^{-1}. (We note, however, that only a preliminary analysis has been conducted of the Doppler spectra, but they are the subject of an ongoing investigation.)

Plate 1 shows the time-height section of the snr. The heights shown along the right ordinate were calculated from the actual zenith angle used, taking the Earth curvature into account. Intense echoes appear between 2130 and 2330 LT above 95 km altitude (150 km range), and between 0400 and 1100 LT at 86–104 km altitude (135–165 km range). The first period corresponds to times just after sunset (2012 LT at 100 km altitude) and the second to times just after sunrise (0344 LT).

The echoes observed during the postsunset period were distributed at higher altitudes and over wider altitude extents than those observed during the postsunrise period. The echoes during the postsunrise period, on the other hand, clearly show more continuous distribution than those during the postsunset period. Although it is easily recognized that the echoes during the postsunset and the postsunrise periods have different morphologies, they both generally show displacements in time toward the radar.

3.2. *Echoes During the Postsunrise Period*

The echoes from the postsunrise period appear continuously from 0400 until 1130 LT at 86–104 km altitude (135–165

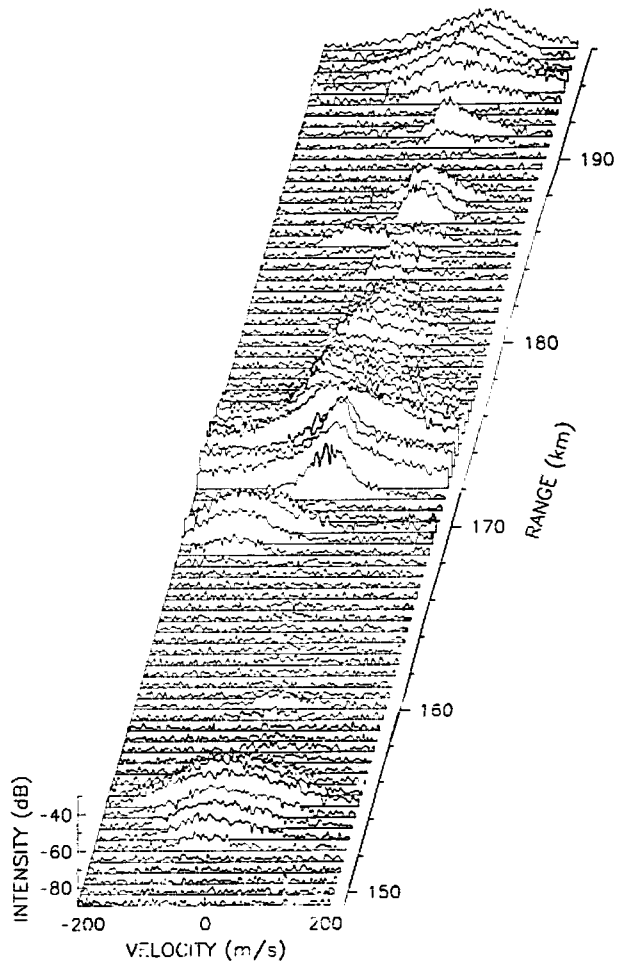

Fig. 1. Doppler spectra associated with backscatter from E region field-aligned irregularities observed in beam 3 at 2140 LT on June 24, 1989.

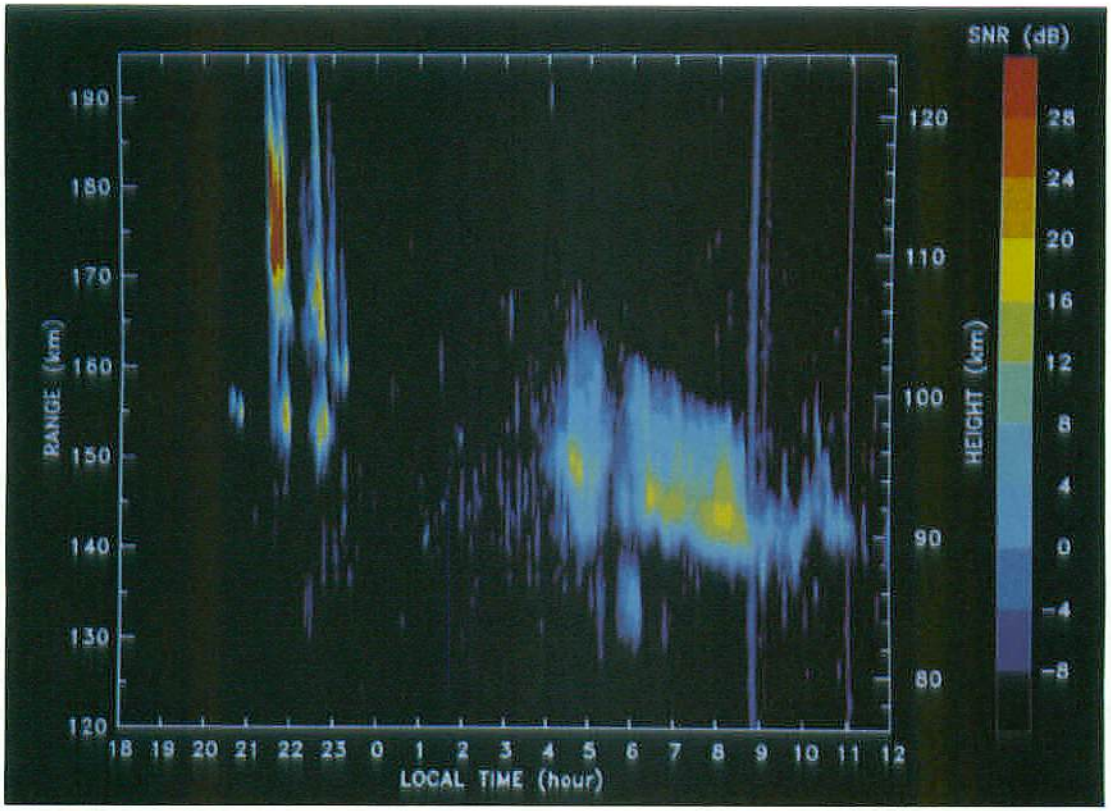

Plate 1. Time-height distribution of echo power observed in beam 3 between 18 LT on June 24, 1989, and 12 LT on June 25, 1989.

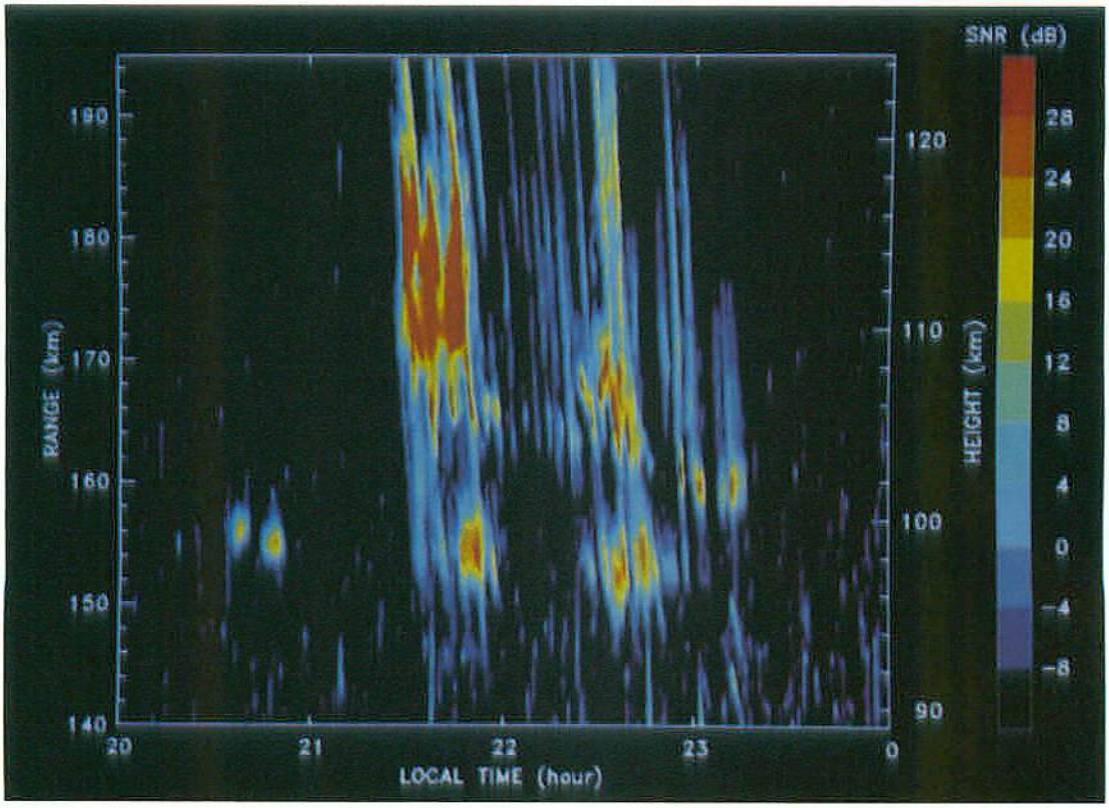

Plate 2. Time-height distribution of echo power observed in beam 3 between 20 LT on June 24, 1989, and 0 LT on June 25, 1989.

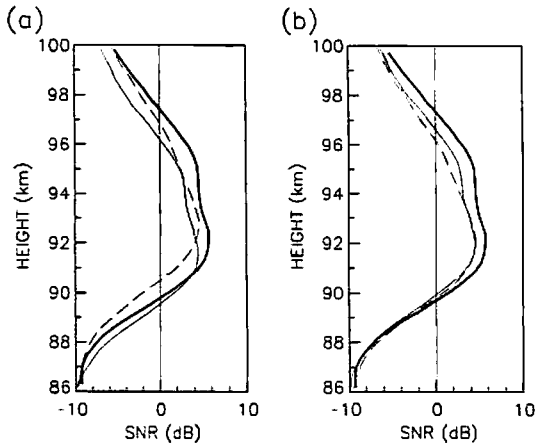

Fig. 2. Height profiles of the echo power averaged over the period from 4–9 LT on June 25, 1989. Thick solid, thin solid, and dashed lines correspond to the data in beams 3, 4, and 5, respectively. (*a*) The height is calculated by using the steered zenith angle shown in Table 1. (*b*) The height is calculated by using the model zenith angle shown in Table 1, which has a direction perpendicular to the geomagnetic field at 100 km altitude.

km range). The intense echoes around 95 km altitude at 5 LT are seen to approach the radar, reaching an altitude around 92 km at 8 LT. This displacement corresponds to a range rate of 0.5 m s^{-1} (0.3 m s^{-1} in altitude).

Figure 2*a* shows the height profiles of the snr in beams 3, 4, and 5 averaged over the period from 4 to 9 LT. The heights were calculated by using the zenith angles of the antenna boresight directions. Although the height distribution shows two broad peaks around 92 and 95 km, the profiles of beams 4 and 5 show slightly different echo power distribution compared with that of beam 3. The echo power profiles for beams 1 and 2 were nearly identical to that for beam 3. Considering the time continuity of the echoes over the averaging period, we might expect measurements from the different beams to produce very similar power profiles. Figure 2*b* shows the same echo power profiles for which the heights were calculated by using the zenith angle obtained from the IGRF85 model for exact perpendicularity to the geomagnetic field line, the "model" zenith angle. Here the echo profiles for all beams agree quite well. We infer from this comparison that the radar returns were coming selectively from the portion of the beam which is perpendicular to the geomagnetic field lines, and the aspect sensitivity is much narrower than the antenna beam width of 4.5°.

The mean Doppler velocities during 6–8 LT are shown in Figure 3. Positive velocity corresponds to motion away from the radar. The plot on the right is a height profile of the mean Doppler velocity averaged in time over the interval 6–8 LT. This averaged velocity is approximately −20 m s^{-1} at the top and bottom of the echo layer, and shows slightly away velocities around 95 km altitude (150 km range). In Plate 1 the echoing region shows a range rate of 0.5 m s^{-1} toward the radar in the period from 5 to 10 LT, which is quite slow compared with the averaged mean Doppler velocity of −20 m s^{-1}.

3.3. *Echoes During the Postsunset Period*

Plate 2 is an expanded segment of Plate 1 displaying the time-height distribution of the snr for the echoes during the postsunset period. Above 100 km altitude, the echoes appear intermittently with a quasi-period of 5–10 min and show rapid and almost constant range rates toward the radar with speeds of 60–90 m s^{-1} (40–60 m s^{-1} in altitude). The most intense echoes appear from 2130 to 2150 LT around 115 km altitude and from 2230 to 2240 LT around 105 km altitude. There are other echoing regions around 98 km altitude at 2030–2050 LT, 2145–2200 LT, and 2230–2250 LT, which occur at altitudes similar to those of the echoes during the postsunrise period, and show gradual displacements toward the radar.

Figure 4 shows the mean Doppler velocities associated with these echo regions. The profile of mean Doppler velocity averaged over 21–23 LT shows a fairly linear change from −20 m s^{-1} at 96 km altitude to 60 m s^{-1} at 120 km altitude. Although the mean Doppler velocities above 102 km altitude are away from the radar, the corresponding range rates of the echoing regions are toward the radar, as shown in Plate 2. Large velocity fluctuations are found with quasi-periods of 5–10 min, which correspond to the range of periodicities found in the intermittent echo power enhancements. The amplitude of the velocity fluctuations sometimes reaches ±40 m s^{-1}, which is much larger than those found in the postsunrise periods. The velocity fluctuations show phase progressions toward the radar, which are associated with motions of the backscattering regions themselves.

The multibeam observations make it possible to measure the horizontal displacements of the echoing regions. Figure 5

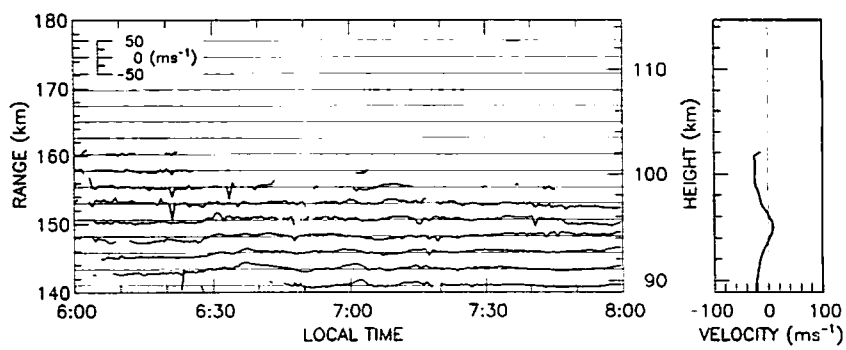

Fig. 3. (Right) Height profile of the mean Doppler velocities averaged over the period from 6 to 8 LT on June 25, 1989. (Left) Fluctuations of the mean Doppler velocities around the averaged values shown by the curve in the right panel. Each time series is averaged over four consecutive ranges. Thin horizontal line corresponds to zero velocity for each range where the velocities are obtained.

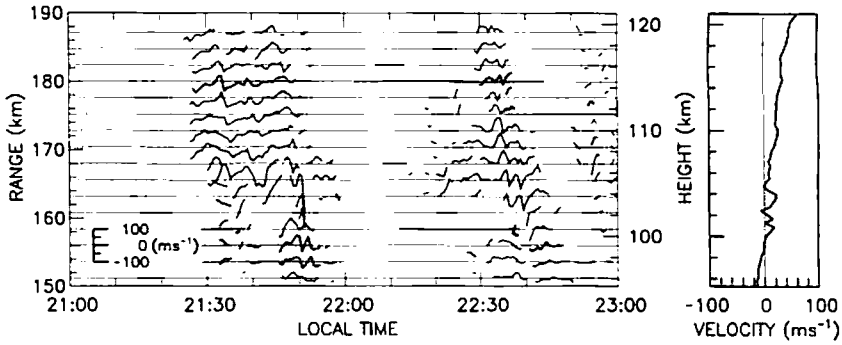

Fig. 4. The same as Figure 3 except that the data are from the period 21–23 LT on June 24, 1989. Note that the scale for the velocity fluctuations is also different from that of Figure 3.

shows contour plots of backscatter strength for the echoes observed in the five different beam directions. The echoes in beam 3 are the same as those shown in Plate 2. During 2125–2150 LT, three intermittent echo power enhancements are apparent with the snr exceeding 25 dB. Although these enhancements show slightly different morphologies from beam to beam, they all appear to maximize in strength around 110 km in altitude. The enhancements appear in the westward beam later than in the eastward beam. Assuming that they are attributed to an identical drifting echoing region, the delay time of 5 min between beam 1 and 5 echoes denotes that the irregularity regions propagated westward with a speed of about 120 m s^{-1}.

4. Discussion and Concluding Remarks

In this paper, we have shown results from MU radar observations of *E* region field-aligned irregularities on June 24–25, 1989. This is the first observation of the *E* region field-aligned irregularities in the mid-latitude region with fine range resolution and with multiple beam directions.

In this case study, we found that echoes observed during periods after sunset and periods after sunrise have quite different morphologies. The echoes during the postsunrise period appear continuously in time and are distributed below 100 km altitude, which we hereinafter call "continuous echoes." The echoes during the postsunset period, on the other hand, appear above 100 km altitude, and show intermittent echo power enhancements with periods of 5–10 min. Hereinafter, we call them "quasi-periodic echoes" for their behavior displayed in the time-height distribution. Almost all echoes during the postsunset period can be classified as quasi-periodic echoes. The echo regions at 96–100 km altitude in the period of 2030–2300 LT, however, resemble the continuous echoes because they did not have large fluctuations of echo power, and were associated with each other to show a slow displacement toward the radar.

Ecklund et al. [1981] and *Riggin et al.* [1986] reported that their *E* region echoes typically occurred between 1830 and 2300 LT above 100 km altitude. *Tanaka and Venkateswaran* [1982*a*] reported a steep rise in the occurrence frequency of the field-perpendicular echoes around 18 LT, which, after a broad maximum around 22 LT, was followed by a gradual decrease until around 6 LT. Our results are consistent with theirs concerning the nighttime prevalence. We, however, appear to be the first to report the 3-m backscatter after sunrise.

In Figure 1, it was found that the spectral width and the mean Doppler velocity of the echoes were similar to those observed by *Ecklund et al.* [1981] and *Tanaka and Venkateswaran* [1982*a*, *b*]. We also infer as others have that the echoes are probably produced by the gradient drift instability acting on electron density gradients related to sporadic *E* layers e.g., as pointed out by *Ecklund et al.* [1981]. In Figure 2, we demonstrated that the backscatter was actually detected in portions of the antenna beam where the line-of-sight direction is perpendicular to the geomagnetic field lines. Although not shown here, this feature was found to be true for both the continuous and the quasi-periodic echoes. We infer that the general altitude distribution of echoing regions can be estimated by the heights given by the right ordinate of each contour map.

As for the mean Doppler velocities, we found that, for both types of echoes, the averaged velocities were not consistent with the range rate of the echoing regions. The mean Doppler velocity represents the line-of-sight motion of the 3.2-m irregularities which is averaged within the scattering volume, while the displacement of echoing regions represents the propagation of regions where irregularities are being generated. The fluctuations in the mean Doppler velocity, on the other hand, were well associated with the types of echoes. The amplitude of the mean Doppler velocity fluctuations for the quasi-periodic echoes was much larger than that for the continuous echoes.

By utilizing the steerability of their radar, *Tanaka and Venkateswaran* [1982*a*] showed the frequent occurrence of westward velocities of 60–80 m s^{-1}. In Figure 5, we found that the regions of the quasi-periodic echoes propagated westward with the speed of 120 m s^{-1}. This is comparable with the results of *Tanaka and Venkateswaran* [1982*a*], but requires further observations.

The main feature of the quasi-periodic echoes is their "striated" distribution in the time-height contour map of the echo power. They propagate toward the radar with a range rate of 60–90 m s^{-1}. We should note that the quasi-periodic echoes have seldom been observed to propagate away from the radar. Although it is difficult to distinguish whether the motion is horizontal or vertical, it is possible that the motion has a downward component. As shown in Figure 4, the mean Doppler velocities for the quasi-periodic echoes showed intense fluctuations with a period that is close to that of the echo power fluctuations. The inward phase propagation of

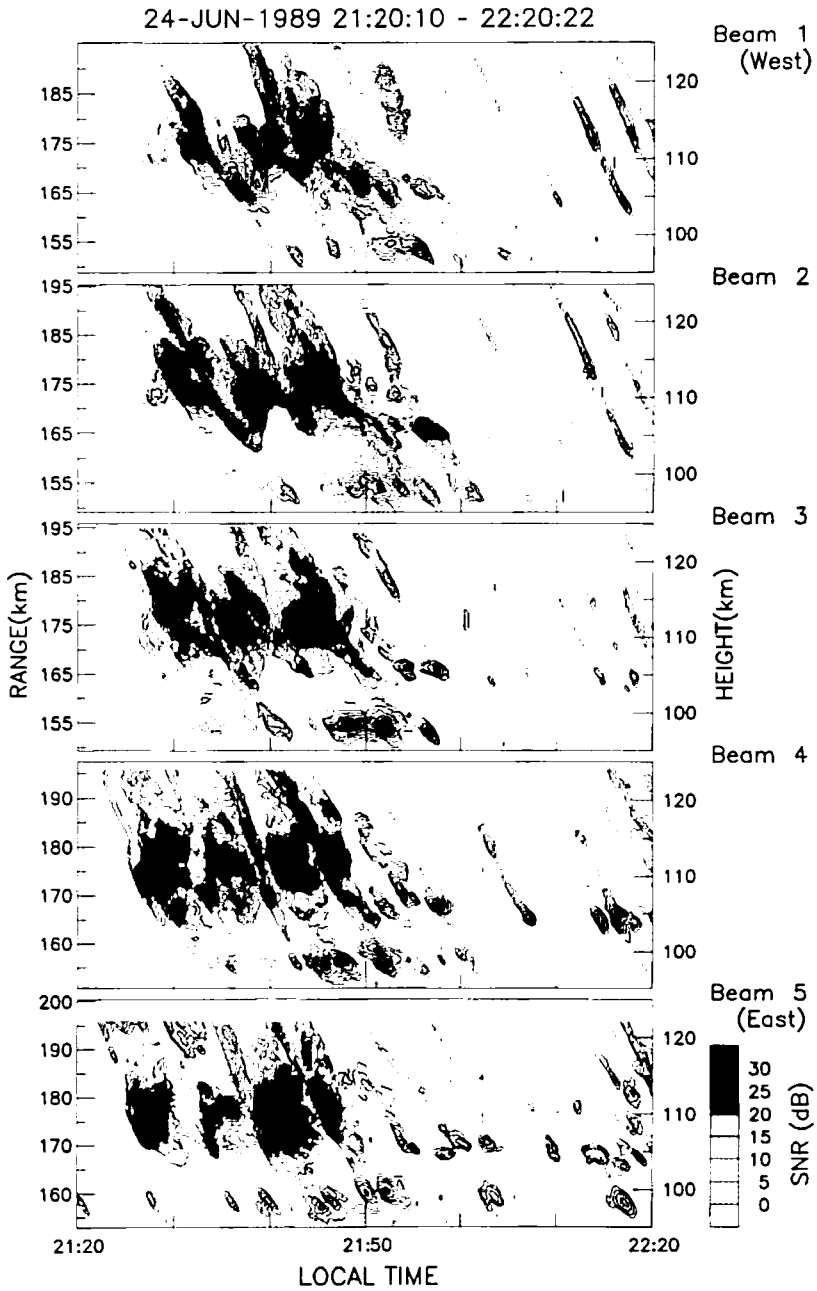

Fig. 5. Time-height distribution of echo power observed in the five different beam directions between 2120 and 2220 LT on June 24, 1989.

the velocity fluctuations was also similar to the range rate of the striated echo power pattern.

Following *Fejer and Kelley* [1980], the gradient drift instability can be most easily developed in the equatorial electrojet where the electrostatic field is vertical, and the vertical electron density gradient is perpendicular to the geomagnetic field. In the mid-latitude region, on the other hand, the perpendicularity between the electron density gradient and the geomagnetic field does not hold. *Kato* [1972] theroretically showed that the gradient drift instability can be generated in the mid-latitude region, although he also mentioned that the short-circuiting effect along the geomagnetic field limits the scale size of such irregularities to less than a few hundred meters. Therefore, while simple theory seems to predict that the gradient drift instability would produce the 3.2-m irregularities detected by the MU radar, it does not predict the periodic nature described here.

Considering that the Brunt-Väisälä period is approximately 5 min in the E region, the striated structures seem to be attributed to the effect of gravity waves in the neutral wind field with periods close to the Brunt-Väisälä period. The range rate of the quasi-periodic echoes is consistent with the downward phase propagation of gravity waves whose energy propagates upward. As shown by *Miller and Smith* [1978], sporadic E layers sometimes show wavelike or distorted structures, which they attributed to gravity waves.

The simple dispersion relation of gravity waves shows that the perturbation velocity makes the angle $\alpha = \sin^{-1}(\omega/\omega_B)$

with respect to the horizontal, where ω and ω_B are the intrinsic frequency of the gravity wave and the Brunt-Väisälä frequency, respectively. Considering that the magnetic dip angle at the MU radar is approximately 50°, a southward propagating gravity wave with the frequency $\omega = \omega_B \sin 50°$ has perturbed velocities which match the direction of the geomagnetic field. Assuming that a thin sporadic E layer is distorted by the inclined wind pattern of the gravity wave, the gravity wave just described would align periodically spaced segments of the sporadic E layer with the geomagnetic field and cause the electron density gradient to become more nearly perpendicular to the geomagnetic field. Since each striated echo layer corresponds to each phase line of the gravity wave, we may find the line striated periodically with the separation equal to the wavelength of the gravity wave. This possible physical mechanism to explain the behavior of the quasi-periodic echoes is more thoroughly discussed by *Woodman et al.* [1991].

Acknowledgments. The authors thank R. T. Tsunoda, W. L. Oliver, and C. A. Reddy for valuable discussions and the careful reading of the manuscript. The MU radar belongs to, and is operated by, the Radio Atmospheric Science Center, Kyoto University.

The Editor thanks B. B. Balsley and B. G. Fejer for their assistance in evaluating this paper.

REFERENCES

Bowles, K. L., B. B. Balsley, and R. Cohen, Field-aligned *E* region irregularities identified with ion acoustic waves, *J. Geophys. Res.*, *68*, 2485–2501, 1963.

Ecklund, W. L., D. A. Carter, and B. B. Balsley, Gradient drift irregularities in mid-latitude sporadic *E*, *J. Geophys. Res.*, *86*, 858–862, 1981.

Fejer, B. G., and M. C. Kelley, Ionospheric irregularities, *Rev. Geophys.*, *18*, 401–454, 1980.

Fukao, S., T. Sato, T. Tsuda, S. Kato, K. Wakasugi and T. Makihira, The MU radar with an active phased array system, 1, Antenna and power amplifiers, *Radio Sci.*, *20*, 1155–1168, 1985*a*.

Fukao, S., T. Tsuda, T. Sato, S. Kato, K. Wakasugi and T. Makihira, The MU radar with an active phased array system, 2, In-house equipment, *Radio Sci.*, *20*, 1169–1176, 1985*b*.

Fukao, S., J. P. McClure, A. Ito, T. Sato, I. Kimura, T. Tsuda, and S. Kato, First VHF radar observation of midlatitude *F*-region field-aligned irregularities, *Geophys. Res. Lett.*, *15*, 768–771, 1988.

Fukao, S., T. Sato, T. Tsuda, M. Yamamoto, M. D. Yamanaka, and S. Kato, The MU radar: New capabilities and system calibrations, *Radio Sci.*, *25*, 477–485, 1990.

Fukao, S., M. C. Kelley, T. Shirakawa, T. Takami, M. Yamamoto, T. Tsuda, and S. Kato, Turbulent upwelling of the mid-latitude ionosphere, 1, Observational results by the MU radar, *J. Geophys. Res.*, *96*, 3725–3746, 1991.

Haldoupis, C., A review on radio studies of auroral *E*-region ionospheric irregularities, *Ann. Geophys.*, *7*, 239–258, 1989.

Kato, S., Cross-field instability for the formation of sporadic *E*, *Radio Sci.*, *7*, 417–423, 1972.

Kato, S., T. Ogawa, T. Tsuda, T. Sato, I. Kimura, and S. Fukao, The middle and upper atmosphere radar: First results using a partial system, *Radio Sci.*, *19*, 1475–1484, 1984.

Kelley, M. C., and S. Fukao, Turbulent upwelling of the mid-latitude ionosphere, 2, Theoretical framework, *J. Geophys. Res.*, *96*, 3747–3753, 1991.

Keys, J. G., and M. K. Andrews, Gravity wave and sporadic-*E* echo signatures on VHF backscatter radar systems, *Planet. Space Sci.*, *32*, 1455–1462, 1984.

Miller, K. L., and L. G. Smith, Incoherent scatter radar observations of irregular structure in mid-latitude sporadic *E* layers, *J. Geophys. Res.*, *83*, 3761–3775, 1978.

Riggin, D., W. E. Swartz, J. Providakes, and D. T. Farley, Radar studies of long-wavelength waves associated with mid-latitude sporadic *E* layers, *J. Geophys. Res.*, *91*, 8011–8024, 1986.

Simon, A., Instability of a partially ionized plasma in crossed electric and magnetic fields, *Phys. Fluids*, *6*, 382–388, 1963.

Tanaka, T., and S. V. Venkateswaran, Characteristics of field-aligned *E*-region irregularities over Iioka (36°N), Japan, I, *J. Atmos. Terr. Phys.*, *44*, 381–393, 1982*a*.

Tanaka, T., and S. V. Venkateswaran, Characteristics of field-aligned *E*-region irregularities over Iioka (36°N), Japan, II, *J. Atmos. Terr. Phys.*, *44*, 395–406, 1982*b*.

Woodman, R. F., M. Yamamoto, and S. Fukao, Gravity wave modulation of gradient drift instabilities in mid-latitude sporadic *E* irregularities, *Geophys. Res. Lett.*, *18*, 1197–1200, 1991.

Yamamoto, M., T. Sato, P. T. May, T. Tsuda, S. Fukao, and S. Kato, Estimation error of spectral parameters of MST radar obtained by least squares fitting method and its lower bound, *Radio Sci.*, *23*, 1013–1021, 1988.

S. Fukao, S. Kato, T. Tsuda, and M. Yamamoto, Radio Atmospheric Science Center, Kyoto University, Uji, Kyoto 611, Japan.

T. Ogawa, Hiraiso Solar Terrestrial Research Center, Communications Research Laboratory, Nakaminato, Ibaraki 311-12, Japan.

R. F. Woodman, Radio Observatorio de Jicamarca, Instituto Geofisico del Peru, Apartado 3747, Lima 100, Peru.

(Received November 8, 1990;
revised April 3, 1991;
accepted April 12, 1991.)